Article

Molecular Puzzle Ring: *pseudo*[1]Rotaxane from a Flexible Cyclodextrin Derivative

Atsuhisa Miyawaki, Paul Kuad, Yoshinori Takashima, Hiroyasu Yamaguchi, and Akira Harada

J. Am. Chem. Soc., **2008**, 130 (50), 17062-17069 • DOI: 10.1021/ja806620z • Publication Date (Web): 19 November 2008

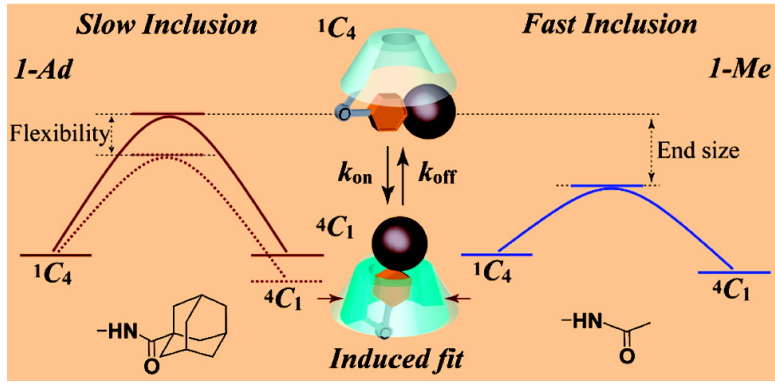

More About This Article

Additional resources and features associated with this article are available within the HTML version:

- Supporting Information
- Access to high resolution figures
- Links to articles and content related to this article
- Copyright permission to reproduce figures and/or text from this article

View the Full Text HTML

J|A|C|S
ARTICLES

Published on Web 11/19/2008

Molecular Puzzle Ring: *pseudo*[1]Rotaxane from a Flexible Cyclodextrin Derivative

Atsuhisa Miyawaki, Paul Kuad, Yoshinori Takashima, Hiroyasu Yamaguchi, and Akira Harada*

Department of Macromolecular Science, Graduate School of Science, Osaka University, Toyonaka, Osaka 560-0043, Japan

Received August 21, 2008; E-mail: harada@chem.sci.osaka-u.ac.jp

Abstract: A *pseudo*[1]rotaxane formed by a flexible cyclodextrin (CD) derivative (**1-R**) with a bulky end group has been investigated on kinetic quantitation. **1-Rs** have the cinnamamide moiety as a guest and a bulky end group (R) as a rate-determining moiety of the threading process. The R groups play an important role for the formation of *pseudo*[1]rotaxane, and kinetics of the self-inclusion process was found to be controlled by the size and shapes of the R groups. **1-Ad** and **1-Me** derivatives, which have an adamantyl and methyl end group, respectively, formed self-inclusion complexes by threading of the arm moiety with a conformational conversion of altrose from $^1C_4$ form to $^4C_1$ form. Flexibility of the *altro*-α-CD cavity resulted in an induced fit (from $^1C_4$ to $^4C_1$) to the arm moiety, and introducing a bulky end group allowed the stability of this *pseudo*[1]rotaxane to be enhanced.

1. Introduction

Aquaporins (AQPs) are nanosize pore channels which express various functions necessary for the maintenance of living systems. AQPs form tetramers as a channel. The size of the pore in the channel is precisely controlled by their peptide sequence and directly affects the molecular transport in the cell membrane, with small pore sizes only allowing small molecules such as water to pass through the pore.[1,2]

Cyclodextrins (CDs), which have a nanosize pore, are well-known to form inclusion complexes with some organic molecules. Significant efforts have been devoted to the investigation of the structures and inclusion properties of CDs.[3−5] When the size of the cavity and structural changes of the host molecules are controlled by specific stimuli, it opens the way to novel applications to new supramolecular systems[6−8] and to AQPs mimic systems where controlling the size of the cavity filters the transported molecules. In an aqueous solution, 3-*mono*-*altro*-α-CD has two equilibrium states ($^1C_4$ and $^4C_1$) due to the altrose moiety where the $^1C_4$ form is thermodynamically more stable than the $^4C_1$ form.[9] However, Fujita et al.[10] and Nolte et al.[11] have reported that the $^4C_1$ form can be stabilized in an inclusion state with the proper guest even if the conformational change from $^1C_4$ to $^4C_1$ occurs with a high energy barrier. Herein, the formation mechanisms of *pseudo*[1]rotaxane are investigated by using *cis*-cinnamamide-*altro*-α-CDs (**1-Rs**) with an adamantyl (Ad), methyl (Me), or trinitrobenzene (TNB) group on the end position of the arms (Scheme 1). The end groups (R) vary in volume with the following order: Ad > TNB ≫ Me.[12] The Ad and TNB groups are often employed as stoppers for α-CD-rotaxane due to being too sterically bulky for the α-CD cavity.[13,14] TNB is the planar structure, but Ad and Me are the spherical structures. The self-assembly and kinetic properties of these compounds are discussed when focusing on the structural properties of the R groups and flexibility of *altro*-α-CD. Upon examination of the induced fit (from $^1C_4$ to $^4C_1$) of the *altro*-α-CD cavity to the arm moiety and comparison with the sizes or shapes of the R groups, both parameters

(1) (a) Agre, P.; Preston, G. M.; Smith, B. L.; Jung, J. S.; Raina, S.; Moon, C.; Guggino, W. B.; Nielsen, S. *Am. J. Physiol. Renal. Physiol.* **1993**, *265*, 463–476. (b) Agre, P. *Angew. Chem., Int. Ed.* **2004**, *43*, 4278–4290.
(2) Gonen, T.; Walz, T. *Q. Rev. Biol.* **2006**, *39*, 361–396.
(3) (a) Szejtli, J. *Chem. Rev.* **1998**, *98*, 1743–1753. (b) Saenger, W.; Katrin Gessler, J. J.; Steiner, T.; Hoffman, D.; Sanbe, H.; Koizumi, K.; Smith, S. M.; Takaha, T. *Chem. Rev.* **1998**, *98*, 1787–1802.
(4) (a) Connors, K. A. *Chem. Rev.* **1997**, *97*, 1325–1357. (b) Rekharsky, M. V.; Inoue, Y. *Chem. Rev.* **1998**, *98*, 1875–1917.
(5) (a) Lipkowitz, K. B. *Chem. Rev.* **1998**, *98*, 1829–1873. (b) Müller, A.; Wenz, G. *Chem. Eur. J.* **2007**, *13*, 2218–2223.
(6) Shinkai, S.; Inuzuka, K.; Miyazaki, O.; Manabe, O. *J. Org. Chem.* **1984**, *49*, 3440–3442.
(7) (a) Hirose, K.; Ishibashi, K.; Shiba, Y.; Doi, Y.; Tobe, Y. *Chem. Lett.* **2007**, *36*, 810–811. (b) Hirose, K.; Shiba, Y.; Ishibashi, K.; Doi, Y.; Tobe, Y. *Chem. Eur. J.* **2008**, *14*, 3427–3433.
(8) Kikuzawa, A.; Kida, T.; Akashi, M. *Org. Lett.* **2007**, *9*, 3909–3912.
(9) Fujita, K.; Ohta, K.; Ikegami, Y.; Shimada, H.; Tahara, T.; Nogami, Y.; Koga, T.; Saito, K.; Nakajima, T. *Tetrahedron. Lett.* **1994**, *35*, 9577–9580.
(10) (a) Fujita, K.; Chen, W.-H.; Yuan, D.-Q.; Nogami, Y.; Koga, T.; Fujioka, T.; Mihashi, K.; Immel, S.; Lichtenthaler, F. W. *Tetrahedron: Asymmetry* **1999**, *10*, 1689–1696. (b) Chen, W.-H.; Fukudome, M.; Yuan, D.-Q.; Fujioka, T.; Mihashi, K.; Fujita, K. *Chem. Commun.* **2000**, *7*, 541–542.
(11) (a) Venema, F.; Nelissen, H. F. M.; Berthault, P.; Birlirakis, N.; Rowan, A. E.; Feiters, M. C.; Nolte, R. J. M. *Chem. Eur. J.* **1998**, *4*, 2237–2250. (b) Birlirakis, N.; Henry, B.; Berthault, P.; Venema, F.; Nolte, R. J. M. *Tetrahedron.* **1998**, *54*, 3513–3522.
(12) Molecular volume and shape of R's were calculated by Spartan'06 software. .
(13) (a) Buston, J. E. H.; Young, J. R.; Anderson, H. L. *Chem. Commun.* **2000**, *11*, 905–906. (b) Tamura, M.; Ueno, A. *Bull. Chem. Soc. Jpn.* **2000**, *73*, 147–154.
(14) (a) Harada, A.; Li, J.; Kamachi, M. *Chem. Commun.* **1997**, *15*, 1413–1414. (b) Easton, J. C.; Lincoln, S. F.; Meyer, A. G.; Onagi, H. *J. Chem. Soc., Perkin Trans.* **1999**, *1*, 2501–2506.

10.1021/ja806620z CCC: $40.75

Scheme 1. Proposed *pseudo*[1]Rotaxane Structures and Chemical Structures of **1-Rs**

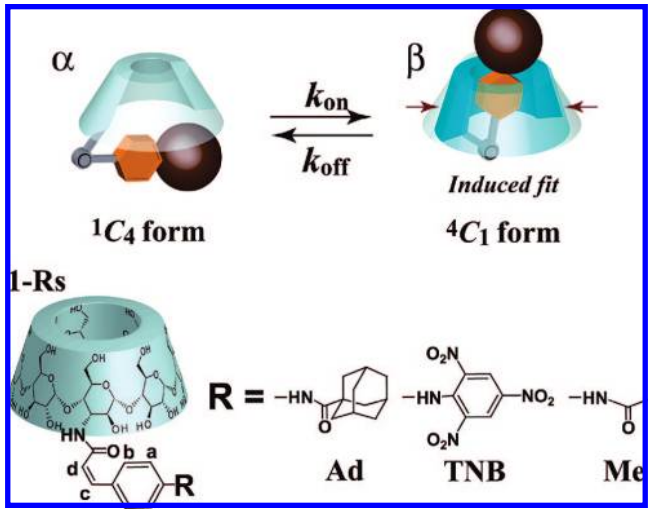

were found to affect the kinetic property of the formation of *pseudo*[1]rotaxanes.

2. Results and Discussion

2.1. Assembly Structure of 1-Ad. The ^{1}H NMR spectrum of **1-Ad** in D_2O differed from that in DMSO-d_6 (Figure 1). In D_2O, two equilibrating species (α and β) were observed in both the aromatic and *altro*-α-CD regions. On the other hand, a single species was observed in DMSO-d_6. These results indicate that **1-Ad** forms a hydrophobicity-driven self-assembly with a complexation rate slower than the NMR time scale at 30 °C in D_2O. The hydrodynamic radii (R_h)[15] of α and β, which were estimated in D_2O using pulsed field gradient spin−echo NMR measurements, were 0.86 (α) and 0.76 (β) nm, suggesting an intramolecular complexation. The NOESY spectrum in D_2O showed correlations between the inner protons of *altro*-α-CD and the protons of the arm moiety assigned to β (Figure 2). A strong correlation between aromatic moiety (protons c_β and d_β) and C5(H), which is located in the narrower rim, was observed, as well as between olefin resonance (b_β) and C3(H), which is located in the wider rim. In contrast, a correlation could not be discerned between *altro*-α-CD and the arm moiety assigned to α. These observations suggest a self-inclusion structure β (Figure 2, right) where the aromatic moiety is included in the *altro*-α-CD cavity but the adamantyl moiety is outside of the narrower rim. Surprisingly, these observations indicate that an Ad group thread through the *altro*-α-CD cavity. In order to understand the detailed inclusion fashion of the aromatic moiety, resonances of *altro*-α-CD were assigned (Figure 3). Drastic upfield and downfield shifts of resonances C3(H) and C5(H) were observed, indicating a strong shielding and deshielding effect produced by the strict inclusion of the aromatic moiety facing its π electron cloud to B and E glucopyranose units (Figure 3, right). Furthermore, the coupling constants of altrose C1(H) in α and β differed (Figure 1, inset). The J_{12} coupling constant assigned to α ($1_\alpha{}^A$) was J_{12} = 6.0 Hz, whereas the constant assigned to β ($1_\beta{}^A$) was J_{12} = 1.5 Hz, indicating the conformational conversion of the altrose from $^1C_4$ to $^4C_1$ through the inclusion process in D_2O.[10,11] The computational investigations suggest that this conformational conversion induces significant distortion of the *altro*-α-CD cavity (see Supporting Information), leading to an induced fit to the arm moiety.

2.2. Size Relations between Ad group and *altro*-α-CD Cavity. A weaker hydrogen-bonding network at secondary hydroxyl side of *altro*-α-CD caused by the introduction of altrose may allow tumbling of the altrose unit of **1-Ad**, leading to the same *pseudo*[1]rotaxane structure described above.[16] Therefore, to confirm the threading of an Ad group through the *altro*-α-CD cavity, the size of an Ad group relative to that of the *altro*-α-CD cavity was experimentally investigated using an axis/wheel system. The axis molecule, both ends of which were capped by the Ad groups, was prepared (Figure 4a). Pyridinium ions were used to improve the solubility in water, and the decamethylene moiety was chosen as a recognition site for α-CD and 3-NH_2-*altro*-α-CD. The axis molecule was mixed with an excess amount of α-CD or 3-NH_2-*altro*-α-CD in D_2O. After reaching the equilibrium of the complexation, the ^{1}H NMR spectrum of the mixture with 3-NH_2-*altro*-α-CD showed both splitting resonances of the axis protons and upfield and downfield shifts of the Ad resonances, whereas the spectrum of the mixture with α-CD only displayed resonance shifts of the Ad protons. This result indicates that both wheel molecules interact with the axis molecule. ROESY measurements were performed to determine the supramolecular structures. The mixture of 3-NH_2-*altro*-α-CD and an axis molecule showed

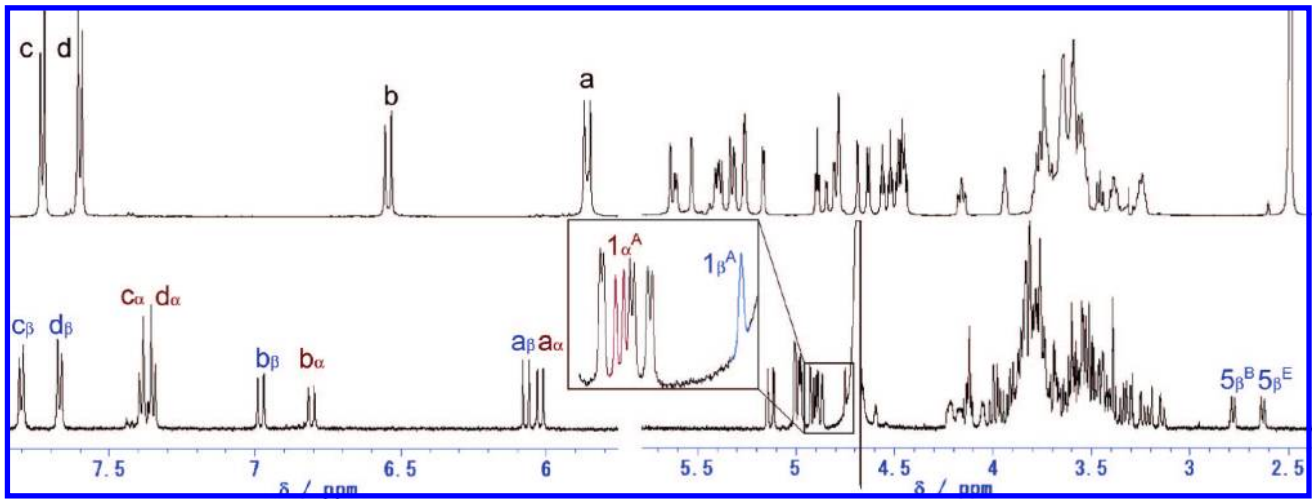

Figure 1. ^{1}H NMR spectra of **1-Ad** at 1 mM in DMSO-d_6 (upper) and D_2O (lower) at 30 °C. Red and blue colors identify resonances assigned to α and β, respectively. Sugar units are labeled clockwise from A to F (viewed from the wider rim), beginning with the altrose unit.

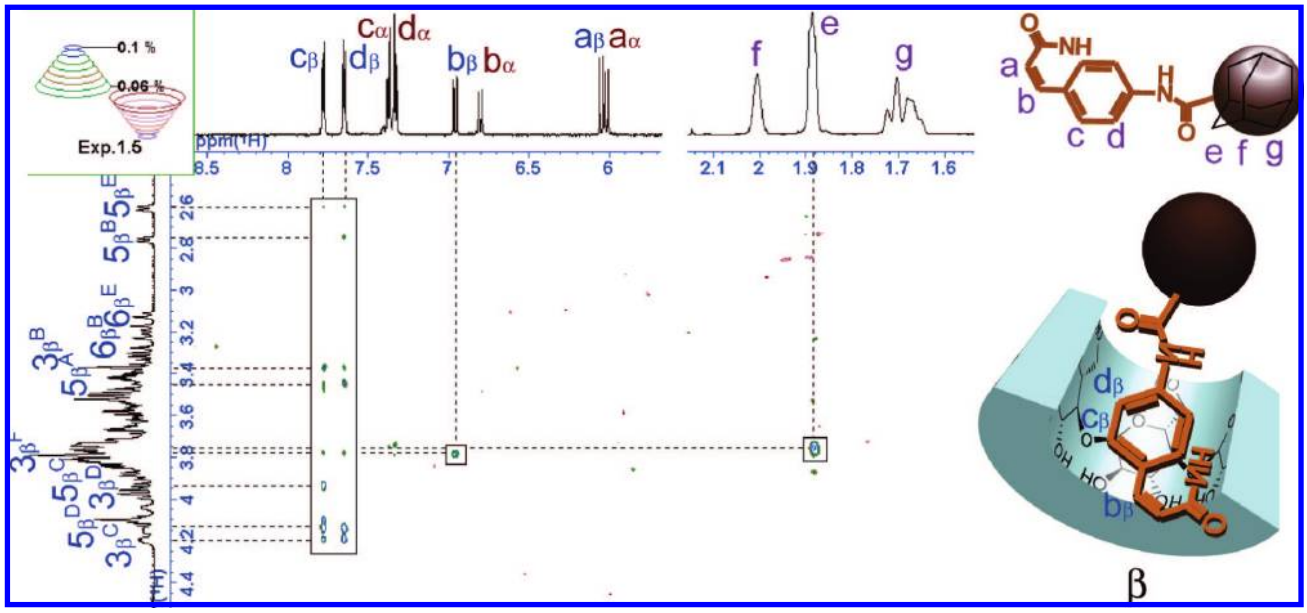

Figure 2. Partial NOESY NMR spectrum of **1-Ad** at 0.5 mM in D_2O (τ_m = 600 ms).

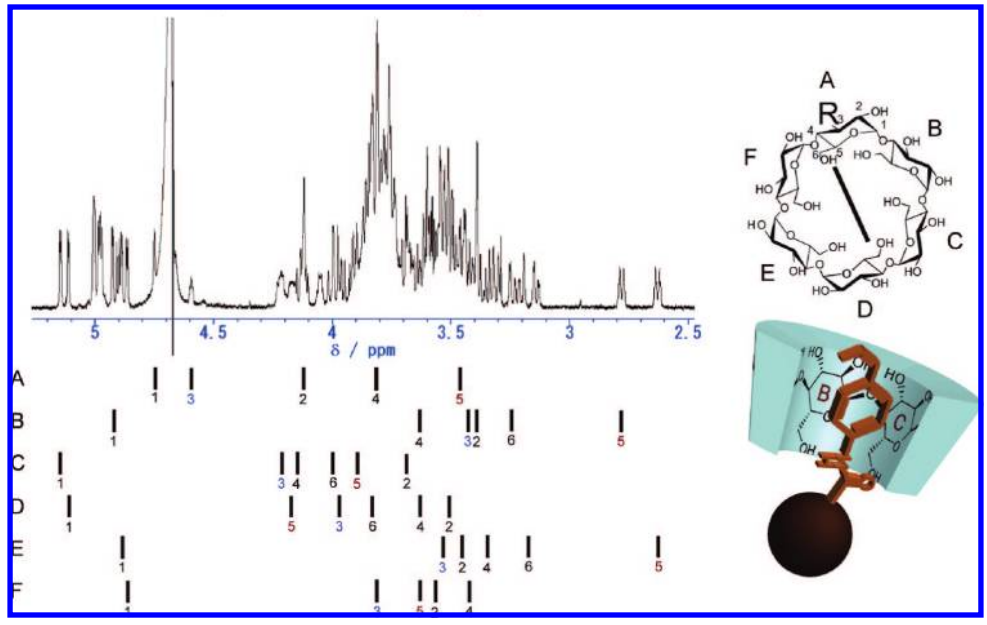

Figure 3. Assignment of the *altro*-α-CD resonances of **1-Ad** based on COSY, TOCSY, ROESY, and HMQC measurements (left) in D_2O, and proposed inclusion fashion of the aromatic moiety (right). Sugar units are labeled clockwise from A to F (viewed from the wider rim), beginning with altrose.

correlations between the inner protons of 3-NH_2-*altro*-α-CD and the protons of both the Ad group and methylene linker (Figure 4b). On the other hand, only a correlation between the inner protons of α-CD and the protons of Ad groups was observed in the mixture with α-CD (Figure 4c). These observations show that 3-NH_2-*altro*-α-CD included both the Ad group and methylene linker moiety, whereas α-CD included only Ad moieties. Conversely, the Ad group can thread through the 3-NH_2-*altro*-α-CD cavity but cannot thread through the α-CD cavity. In conclusion, *altro*-α-CD has a cavity large enough to allow threading of the Ad group due to the introduction of the altrose moiety.

2.3. Assembly Structures of 1-Me and 1-TNB. The self-assembly properties of **1-Me** and **1-TNB** were also investigated in D_2O. The arrangement of the ^1H NMR resonances of **1-Me** was similar to that of **1-Ad** because two equilibrating species (α and *β*) with different J_{12} values ($J_{12(\alpha)}$ = 6.0 and $J_{12(\beta)}$ 1.5 Hz) were observed (Figure 5b). The spectral property of **1-Me**, such as R_h values ($R_{h(\alpha)}$ = 7.8 nm and $R_{h(\beta)}$ = 7.3 nm), anisotropic effects to C3(H) and C5(H) protons, and ROESY analysis, are similar to those of **1-Ad**, suggesting the intramolecular complexation and strict inclusion of the aromatic moiety. On the other hand, **1-TNB** showed a single-species resonance with a J_{12} value of 6.3 Hz, indicative of the $^1C_4$ form (Figure

(15) The R_h values were calculated by using the Stokes−Einstein equation.
(16) (a) Chen, Z.; Bradshaw, S, J.; Yi, G.; Pyo, D.; Black, R, D.; Zimmerman, S. S.; Lee, L. M. *J. Org. Chem.* **1996**, *61*, 8949–8955. (b) Yamada, T.; Fukuhara, G.; Kaneda, T. *Chem. Lett.* **2003**, *32*, 534–535. (c) Nishiyabu, R.; Kano, K. *Eur. J. Org. Chem.* **2004**, *24*, 4985–4988.

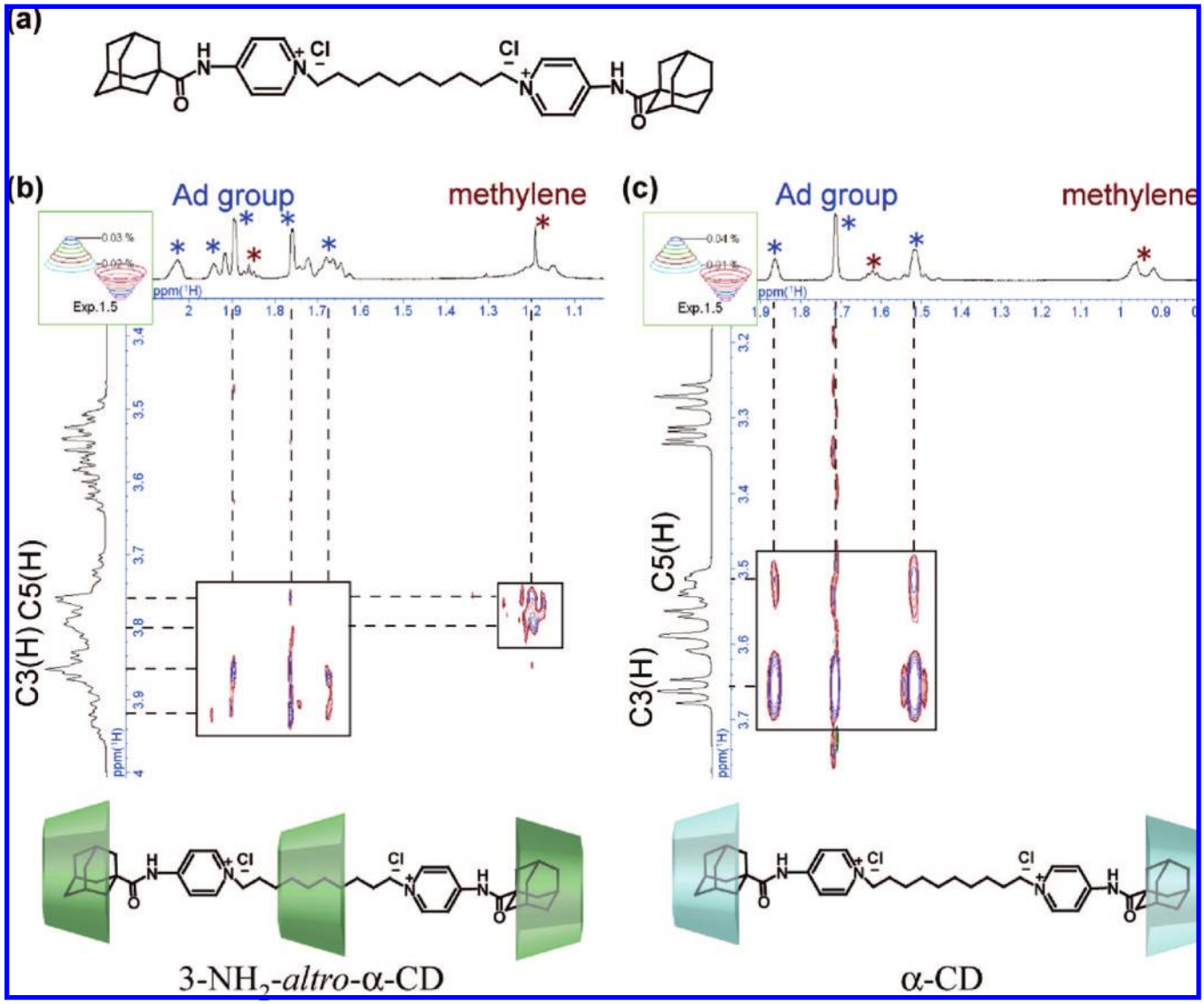

Figure 4. Chemical structure of the axis molecule (a). Partial ROESY spectrum of the mixture of axis molecule (1.25 mM) and 3-NH_2-*altro*-α-CD (10 mM) at τ_m = 200 ms in D_2O (b), and the mixture of axis molecule (1.25 mM) and α-CD (10 mM) at τ_m = 200 ms in D_2O (c), respectively.

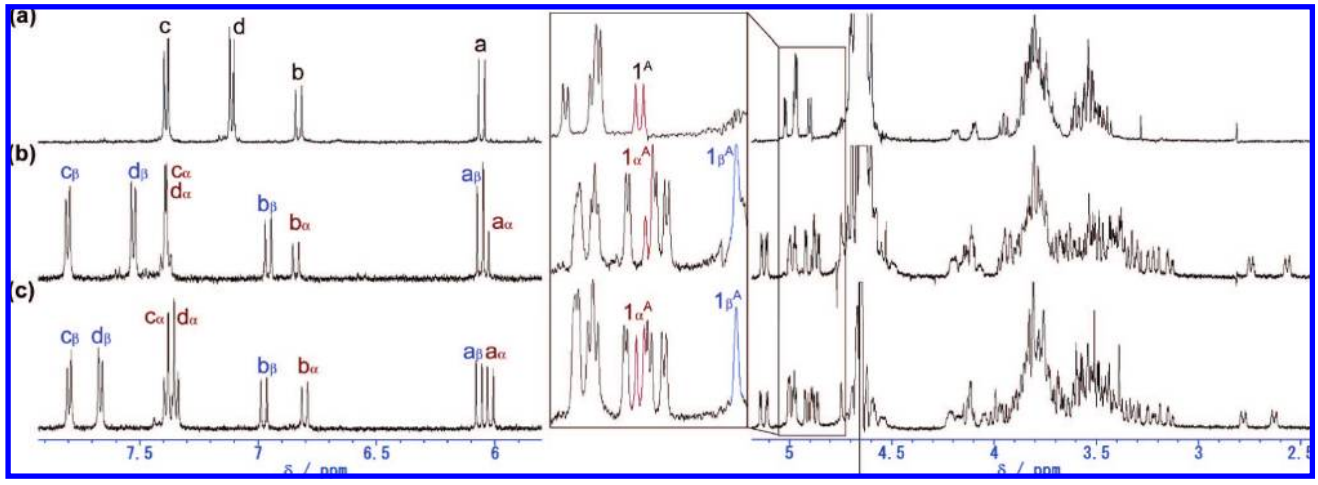

Figure 5. ^{1}H NMR spectra of (a) **1-TNB**, (b) **1-Me**, and (c) **1-Ad** in D_2O at 30 °C.

5a). No correlation could be discerned between *altro*-α-CD and the arm moiety in any mixing time (τ_m = 150, 200, and 600 ms) in ROESY analysis, suggesting the noninclusion form. On the basis of these results, it was concluded that **1-Me** forms a self-inclusion complex similar to that formed by **1-Ad**, whereas **1-TNB** cannot form such a complex. Hence, we hypothesize

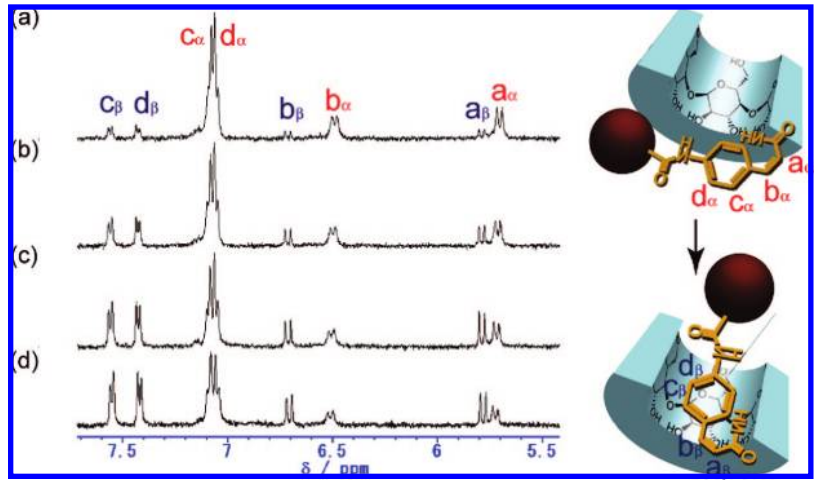

Figure 6. Time course ^{1}H NMR spectra of **1-Ad** (5 °C, 1 mM, D_2O) 210 s (a), 1590 s (b), 3279 s (c), and saturated state (d).

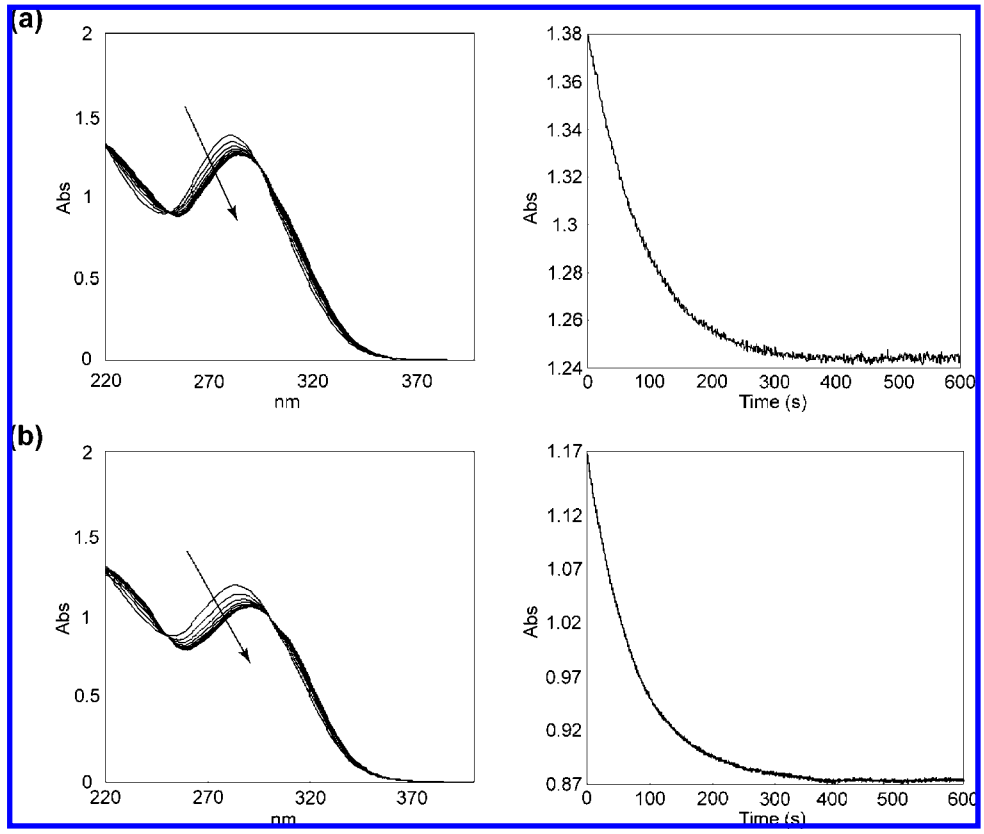

Figure 7. Time course UV−vis spectra of **1-Ad** (left) and its absorbance decay at 280 nm (right) in pH = 7 (a) and in pH > 12 (b).

that the end group plays an important role for self-complexation and that the planarity of the TNB group is not suitable for threading through the *altro*-α-CD cavity.

2.4. Kinetic Investigation. The formation mechanism of these assemblies was kinetically investigated. **1-Ad** and **1-Me** formed self-inclusion complexes by way of the threading of the arm moiety with a conformational conversion of the altrose. Neither a coalescence tendency of resonances nor chemical exchange signals were observed between the α and *β* resonances of **1-Ad** in the NMR analysis, indicating that **1-Ad** did not interconvert on the NMR time scale ($10^{-2} < k < 10^2$ s^{-1}) at 30 °C. The initial and final structures of **1-Ad** in this interconversion were confirmed by the time course ^{1}H NMR experiment at low temperature (Figure 6). The integral of the resonances assigned to *β* increased with time, whereas that of the resonances assigned to α decreased, indicating the interconversion between noninclusion (α) and inclusion (*β*). This result suggests that the initial structure was mainly in its noninclusion form and that the ratio of the self-inclusion form gradually increased as a function of time (s) in aqueous solutions.

To determine the rate constant (*k*) of such a slow interconversion, time course UV−vis measurements for **1-Ad** were performed in water. A UV−vis experiment is suitable for the quantitative investigation of its kinetics at room temperature. The absorbance of **1-Ad** was measured as soon as the compound prepared by precipitation from methanol to acetone was dissolved in water until equilibrium was reached (Figure 7a, left). Figure 7a, right shows the absorbance decay at 280 nm

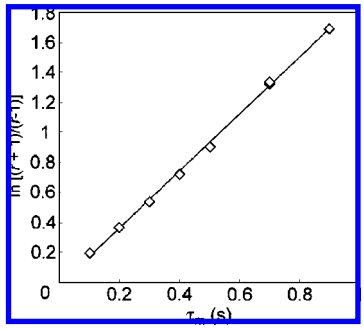

Figure 8. Results of EXSY measurement for **1-Me**. Plots of $\ln[(r+1)/(r-1)]$ as a function of mixing time (τ_m = 100, 200, 300, 400, 500, 700, and 900 ms).

and its saturation after 600 s. The time course UV−vis experiment for **1-Rs** also reveals that no other processes (hydration, local heat effect of dissolving sample) produce spectral change in the experimental time scale. Therefore, we concluded that this absorbance decay indicates the environmental variations around the aromatic moiety such as hydration and electron density change related to the inclusion of aromatic moiety into the *altro*-α-CD cavity. The k values for the interconversion between noninclusion and self-inclusion of **1-Ad** were determined to be 5.9×10^{-3} s^{-1} using a first-order opposing equation, which corresponds to a free energy of activation ($\Delta G_{on,off}^{\ddagger}$) of 87.2 kJ mol^{-1} at 30 °C. This k value is reasonable because this rate constant is out of the range of EXSY experiments. On the other hand, **1-Me** did not show such UV decay because of a faster interconversion (see Supporting Information). Therefore, rate constants for the interconversion of **1-Me** were estimated by using chemical exchange signals between the α and the β resonances in EXSY measurements (Figure 8).

Table 1 lists the determined k values from UV−vis and EXSY analysis. It should be noted that the k values of **1-Ad** are 100−200 times smaller than those of **1-Me**. These differences in the free energy of activation ($\Delta[\Delta G_{on,off}^{\ddagger}] = 12$ and 13.4 kJ mol^{-1}) imply an energy barrier for the puzzle ring structure of **1-Ad** derived from the relation between the size of an Ad group and the flexibility of the *altro*-α-CD cavity. In order to further understand the flexibility contribution of *altro*-α-CD in the assembly process of **1-Ad**, the k values were determined under deprotonated conditions of the hydroxyl groups because CDs have rigid structures aided by intramolecular hydrogen bonding between the hydroxyl groups[3] (Figure 7b). The $\Delta G_{on}^{\ddagger}$ value in basic conditions is listed in Table 1, and shows a decrement of free energy of activation ($\Delta[\Delta G_{on}^{\ddagger}] = 1.6$ kJ mol^{-1}). The free energy ($-\Delta G^{o}$) estimated by van't Hoff plots also shows thermodynamic stabilization of *pseudo*[1]rotaxane under deprotonated conditions. These results suggest that the flexibility of the cyclodextrin framework is advantageous to form *pseudo*[1]rotaxane from both kinetic and thermodynamic points of view, indicating the effect of intramolecular hydrogen bonding on the flexibility of *altro*-α-CD.

3. Conclusions

1-Rs having the cinnamamide moiety as a guest and bulky end groups as a rate-determining moiety of the threading process have been prepared, and their supramolecular structures and kinetic properties have been quantitatively examined. Kinetics of the self-inclusion process was found to be controlled by the size and shape of the R groups. These results suggest that the self-inclusion process does not derive from tumbling of the altrose unit bearing the arm moiety, but by threading of the arm moiety through the CD cavity.

It is concluded that **1-Ad** forms a *pseudo*[1]rotaxane with a higher $\Delta G_{on,off}^{\ddagger}$ than **1-Me**. The Ad group is an important component for this assembly process, and modification of pyranose from glucopyranose to altropyranose enables the Ad group to thread through the *altro*-α-CD cavity. We speculate that the flexibility of *altro*-α-CD results in an induced fit, which enhances the stability of this *pseudo*[1]rotaxane with the Ad group, and leads to this unexpected result.

4. Experimental Section

4.1. Materials. α-Cyclodextrin (α-CD) was obtained from Junsei Chemical Co., Ltd. *trans-p*-Aminocinnamic acid, 4-aminopyridine, and 1,10-diiododecane were obtained from Tokyo Kasei Kogyo, Co., Ltd. *N*,*N*′-Dicyclohexylcarbodiimide (DCC), 1-hydroxybenzotriazole (1-HOBt), acetic anhydride, and 2,4,6-trinitrobenzenesulfonic acid sodium salt were obtained from Nacalai Tesque Inc. Dimethyl sulfoxide-d_6 (DMSO-d_6), and D_2O used as solvents for NMR measurements were obtained from Merck Ltd. 3A-Amino-3A-deoxy-(2AS,3AS)-α-CD (3-NH_2-*altro*-α-CD) was prepared according to the method reported previously.[17]

4.2. Synthesis. 4.2.1. Preparation of 1-Ad and 1-Me. 1-Rs (**1-Ad** and **1-Me**) were prepared by photo irradiation of the *trans*-cinnamamide-*altro*-α-CD derivatives (***trans*1-Ad** and ***trans*1-Me**) using xenon light source and optical filters (center wavelength: 300 nm, half-bandwidth: 10 nm) with further purification by HPLC.

4.2.1.1. 1-Ad. *trans*1-Ad was prepared according to the method reported previously[18] and was dissolved in methanol (100 mg/50 mL). After the photo irradiation (λ = 300 nm), the solution was evaporated. The precipitate was purified by HPLC to give **1-Ad** in 32% yield.

^{1}H NMR (DMSO-d_6, 600 MHz): δ 9.16 (s, 1H, N*H*), 8.03 (d, J = 9.0 Hz, 1H, N*H*), 7.73 (d, J = 8.7 Hz, 2H of *Ph*), 7.60 (d, J = 8.7 Hz, 2H of *Ph*), 6.54 (d, J = 13.0 Hz, 1H, PhC*H*═), 5.86 (d, J = 13.0 Hz, 1H, ═C*H*CO), 5.64−5.16 (m, 11H, O(2)*H*, and O(3)*H* of α-CD), 4.89 (t, J = 5.2 Hz, 2H, C(6′)*H* of α-CD), 4.85−4.63 (m, 5H, C(1)*H* of α-CD), 4.64 (d, J = 6.7 Hz, 1H C(1′)*H* of α-CD), 4.56−4.44 (m, 10H, O(6)*H* of α-CD), 4.16 (m, 1H, C(3′)*H* of α-CD), 3.94 (m, 1H, C(5′)*H* of α-CD), 3.78−3.55 (m, 12H, C(4′)*H*, C(3)*H*, C(5)*H* and C(2′)*H* of α-CD), 3.47−3.24 (m, 10H, C(4)*H* and C(2)*H* of α-CD), 2.01(s, 3H, −C*H*−), 1.90(s, 6H, −CH−CH_2−C−), 1.69 (s, 6H, −CH−CH_2−CH−). Positive ion MALDI-TOF Mass m/z = 1303 $[M + Na]^+$. Elemental Anal. Calcd for $C_{56}H_{82}N_2O_{31}\cdot 7.2H_2O$: C, 47.74; H, 6.90; N, 1.99. Found: C, 47.38; H, 6.53; N, 2.00.

4.2.1.2. 1-Me. 4.2.1.2.1. *p*-Methylamidecinnamic acid (MeAmCiOH). To a solution of *trans-p*-aminocinnamic acid (1.0 g, 6.1 mmol) in methanol was added acetic anhydride (2 mL). After stirring the methanol solution at room temperature for 3 h, the

Table 1. Kinetic Parameters of **1-Ad** and **1-Me**.

1-Rs	pH	method	τ^{-1} [s^{-1}]	k_{on} [s^{-1}]	$\Delta G_{on}^{\ddagger}$ [kJ mol^{-1}]	k_{off} [s^{-1}]	$\Delta G_{off}^{\ddagger}$ [kJ mol^{-1}]	K	ΔG^{o} [kJ mol^{-1}]
1-Ad	7	UV	1.17×10^{-2}	5.9×10^{-3}	87.2	5.9×10^{-3}	87.2	1.0	−0.1
1-Ad	>12	UV	1.34×10^{-2}	1.1×10^{-2}	85.6	2.4×10^{-3}	89.4	4.5	3.8
1-Me	7	NMR	1.89	1.2	73.8	6.8×10^{-1}	75.2	1.8	1.4

solution became turbid gradually. The precipitate was collected by filtration and washed with NaOH aqueous solution (pH = 11) to give MeAmCiOH in 79% yield.

^{1}H NMR (DMSO-d_6, 500 MHz): δ 12.20 (s, 1H COO*H*), 10.09 (s, 1H, N*H*), 7.60 (s, 4H of *Ph*), 7.50 (d, J = 16.0 Hz, 1H Ph−C*H*═), 6.39 (d, J = 16.0 Hz, 1H, ═C*H*CO), 2.05 (s, 3H, −COCH_3).

4.2.1.2.2. *trans*1-Me. To a solution of 3-NH_2-*altro*-α-CD (200 mg, 0.21 mmol) in 20 mL DMF was added MeAmCiOH (51 mg, 0.25 mmol). After the solution was cooled down below 0 °C, DCC (51 mg, 0.25 mmol) and 1-HOBt (33 mg, 0.25 mmol) were added. The resulting mixture was stirred at room temperature for 5 days. After insoluble materials were removed by filtration, the filtrate was poured into acetone (250 mL). The precipitate was purified by preparative reversed phase chromatography (elution: water-acetonitrile) to give ***trans*1-Me** in 46% yield.

^{1}H NMR (DMSO-d_6, 500 MHz): δ 10.05 (s, 1H, -N*H*), 8.10 (d, J = 9.3 Hz, 1H, −N*H*), 7.71 (d, J = 8.6 Hz, 2-H of *Ph*), 7.55 (d, J = 8.6 Hz, 2-H of *Ph*), 7.34 (d, J = 15.6 Hz, 1H, Ph−C*H*═), 6.44 (d, J = 15.6 Hz, 1H, ═C*H*−CO), 5.94−5.15 (m, 11H, O(2)*H*, and O(3)*H* of α-CD), 4.87 (t, J = 5.2 Hz, 2H, C(6′)*H* of α-CD), 4.85−4.77 (m, 5H, C(1)*H* of α-CD), 4.65 (d, J = 6.6 Hz, 1H, C(1′)*H* of α-CD), 4.53−4.41 (m, 10H, O(6)*H* of α-CD), 4.16 (m, 1H, C(3′)*H* of α-CD), 3.88 (m, 1H, C(5′)*H* of α-CD), 3.81−3.56 (m, 12H, C(4′)*H*, C(3)*H*, C(5)*H* and C(2′)*H* of α-CD), 3.45−3.20 (m, overlaps with HOD), 2.05 (s, 3H, −CH_3). Positive ion MALDI-TOF Mass m/z = 1154 [M + Na]$^+$.

4.2.1.2.3. *cis*1-Me. ***trans*1-Me** was dissolved in methanol (0.11 g/30 mL). After the photo irradiation (λ = 300 nm), the solution was evaporated. The precipitate was purified by HPLC to give **1-Me** in 61% yield.

^{1}H NMR (DMSO-d_6, 500 MHz): δ 9.98 (s, 1H, N*H*), 8.00 (d, J = 9.3 Hz, 1H, N*H*), 7.72 (d, J = 8.9 Hz, 2H of *Ph*), 7.50 (d, J = 8.9 Hz, 2H of *Ph*), 6.55 (d, J = 13.0 Hz, 1H, PhC*H*═), 5.87 (d, J = 13.0 Hz, 1H, ═C*H*CO), 5.84−5.14 (m, 11H, O(2)*H*, and O(3)*H* of α-CD), 4.87 (t, J = 5.3 Hz, 2H, C(6′)*H* of α-CD), 4.85−4.66 (m, 5H, C(1)*H* of α-CD), 4.64 (d, J = 6.7 Hz, 1H C(1′)*H* of α-CD), 4.54−4.41 (m, 10H, O(6)*H* of α-CD), 4.16 (m, 1H, C(3′)*H* of α-CD), 3.93 (m, 1H, C(5′)*H* of α-CD), 3.78−3.55 (m, 12H, C(4′)*H*, C(3)*H*, C(5)*H* and C(2′)*H* of α-CD), 3.48−3.35 (m, 10H, C(4)*H* and C(2)*H* of α-CD), 2.03 (s, 3H, −CH_3). Positive ion MALDI-TOF Mass m/z = 1154 [M + Na]$^+$. Elemental Anal. Calcd for $C_{47}H_{70}N_2O_{31}\cdot 7H_2O$: C, 43.93; H, 6.59; N, 2.18. Found: C, 44.06; H, 6.31; N, 2.18.

4.2.2. Preparation of 1-TNB. 4.2.2.1. *cis*−*trans* Mixture of *p*-Aminocinnamic Acid (*cis*−*trans*-AmCiOH). *trans-p*-Aminocinnamic acid was dissolved in methanol (205 mg/25 mL). After the photo irradiation (λ = 300 nm), the solution was evaporated. The ratio of the isomerization was determined by using ^{1}H NMR measurement (*cis*/*trans* = 0.85).

^{1}H NMR (DMSO-d_6, 500 MHz): δ 11.80 (s, 2H *cis*- and *trans*COO*H*), 7.59 (d, J = 8.6 Hz, 2H of *cisPh*), 7.40 (d, J = 15.8 Hz, 1H *trans*Ph−C*H*═), 7.32 (d, J = 8.6 Hz, 2H, *transPh*), 6.63 (d, J = 13.0 Hz, 1H *cis*Ph−C*H*═), 6.54 (d, J = 8.6 Hz, 2H, *transPh*), 6.50 (d, J = 8.6 Hz, 2H of *cisPh*), 6.11 (d, J = 15.8 Hz, 1H *trans* = C*H*CO), 5.67 (s, 2H *trans*NH_2), 5.57 (s, 2H *cis*NH_2), (s, 3H, −COCH_3), 5.52 (d, J = 13.0 Hz, 1H *cis* = C*H*CO).

4.2.2.2. *cis*−*trans* Mixture of *p*-Trinitrophenylaminocinnamic Acid (*cis*−*trans*-TNBAmCiOH). To a solution of *cis*−*trans*AmCiOH (0.15 g, 0.94 mmol) in 25 mL of NaOH aqueous solution was added trinitrobenzene sulfonic acid sodium salt (0.40 g, 1.1 mmol). After the solution was stirred at room temperature for 5 h, the solution pH was adjusted to 2−3 by using hydrochloric acid. The precipitate was dissolved in ethyl acetate and washed with hydrochloric acid. The ethyl acetate phase was evaporated to give *cis*−*trans*TNBAmCiOH in 63% yield.

^{1}H NMR (DMSO-d_6, 500 MHz): δ 12.28 (s, 1H COO*H*), 10.21 (s, 1H *trans*N*H*), 10.19 (s, 1H *cis*N*H*), 8.96 (s, 2H of *transPh*), 8.95 (s, 2H of *cisPh*), 7.63 (d, J = 8.6 Hz, 4H of *cis*- and *transPh*), 7.53 (d, J = 16.0 Hz, 1H *trans*Ph−C*H*═), 7.16 (d, J = 8.6 Hz, 2H of *transPh*), 7.12 (d, J = 8.6 Hz, 2H of *cisPh*), 6.83 (d, J = 12.8 Hz, 1H *cis*Ph−C*H*═), 6.46 (d, J = 16.0 Hz, 1H *trans* = C*H*CO), 5.91 (d, J = 12.8 Hz, 1H *cis* = C*H*CO).

4.2.2.3. *cis*1-TNB. To a solution of 3-NH_2-*altro*-α-CD (0.57 g, 0.6 mmol) in 50 mL DMF was added *cis-trans*TNBAmCiOH (0.22 g, 0.6 mmol). After the solution was cooled down below 0 °C, DCC (0.15 mg, 0.72 mmol) and 1-HOBt (95 mg, 0.72 mmol) were added. The resulting mixture was stirred at room temperature for 5 days. After insoluble materials were removed by filtration, the filtrate was poured into acetone (500 mL). The precipitate was purified by preparative reversed phase chromatography (elution: water−acetonitrile) to give ***cis*1-TNB** in 13% yield.

^{1}H NMR (DMSO-d_6, 500 MHz): δ 10.19 (s, 1H, N*H*), 8.94 (s, 2H of *Ph*), 8.06 (d, J = 8.7 Hz, 1H, N*H*), 7.77 (d, J = 8.5 Hz, 2H of *Ph*), 7.06 (s, 2H of *Ph*), 6.58 (d, J = 12.7 Hz, 1H, PhC*H*═), 5.92 (d, J = 12.7 Hz, 1H, ═C*H*CO), 5.84−5.17 (m, 11H, O(2)*H*, and O(3)*H* of α-CD), 4.87 (t, J = 5.3 Hz, 2H, C(6′)*H* of α-CD), 4.85−4.71 (m, 5H, C(1)*H* of α-CD), 4.64 (d, J = 6.8 Hz, 1H C(1′)*H* of α-CD), 4.55−4.43 (m, 10H, O(6)*H* of α-CD), 4.16 (m, 1H, C(3′)*H* of α-CD), 3.94 (m, 1H, C(5′)*H* of α-CD), 3.75−3.55 (m, 12H, C(4′)*H*, C(3)*H*, C(5)*H* and C(2′)*H* of α-CD), 3.46−3.39 (m, 10H, C(4)*H* and C(2)*H* of α-CD). Positive ion MALDI-TOF Mass m/z = 1322 [M + Na]$^+$. Elemental Anal. Calcd for $C_{51}H_{69}N_5O_{36}\cdot 6H_2O$: C, 42.65; H, 5.68; N, 4.88. Found: C, 42.25; H, 5.49; N, 4.92.

4.2.3. Preparation of the Axis Molecule. 4.2.3.1. 4-Adamantylamidepyridine (AdPy). To a solution of 4-aminopyridine (1.0 g, 10.6 mmol) and triethylamine (1.0 g, 9.9 mmol) in 80 mL of THF was added 1-adamantanecarbonyl chloride (1.7 g, 8.5 mmol) in 15 mL of THF solution under ice cooling. The resulting mixture was stirred at room temperature overnight. After the precipitate was removed, the solution phase was concentrated and dissolved in ethylacetate. The solution was washed with hydrochloric acid (pH = 3) and was evaporated to give **AdPy** in 62% yield.

^{1}H NMR (DMSO-d_6, 500 MHz): δ 9.44 (s, 1H, N*H*), 8.38 (d, J = 6.3 Hz, 2H of *Py*), 7.68 (d, J = 6.3 Hz, 2H of *Py*), 2.01 (s, 3H, −C*H*−), 1.90 (s, 6H, −CH_2−), 1.70 (s, 6H, −CH_2−).

4.2.3.2. Bis(4-adamantylamidepyridine)decane ([AdPy-C10-PyAd]$^{2+}\cdot$2Cl$^-$). The acetonitrile solution of AdPy (0.80 g, 3.1 mmol) and 1,10-diododecane (0.74 g, 1.9 mmol) was stirred under reflux for 3 days. The precipitate was collected and washed with acetonitrile to give **[AdPy-C10-PyAd]$^{2+}\cdot$2I$^-$** in 31% yield. A saturated aqueous solution of **[AdPy-C10-PyAd]$^{2+}\cdot$2I$^-$** was poured into an aqueous solution of hexafluorophosphate ammonium, and the solution was stirred for 2 days at room temperature. The precipitate was collected by centrifugal separation and washed with water to give **[AdPy-C10-PyAd]$^{2+}\cdot$2PF$_6^-$** in 90% yield. An acetone solution of **[AdPy-C10-PyAd]$^{2+}\cdot$2PF$_6^-$** was poured into an acetone solution of tetraethylammonium chloride, and the solution was stirred for 2 days at room temperature. The precipitate was collected by centrifugal separation and washed with acetone to give **[AdPy-C10-PyAd]$^{2+}\cdot$2Cl$^-$** in 89% yield.

^{1}H NMR (D_2O, 500 MHz): δ 8.50 (d, J = 7.5 Hz, 4H of *Py*), 8.09 (d, J = 7.5 Hz, 4H of *Py*), 4.65 (t, J = 7.1 Hz, 4H, α-methylene in decamethylene), 2.00 (s, 6H, methyne in Ad), 1.87 (s, 12H, methylene in Ad), 1.85 (m, 4H, β methylene in decamethylene), 1.68 (q, J = 11.6 Hz and 22.9 Hz, 12H, methylene in Ad), 1.21−1.14 (m, methylene in decamethylene). Elemental Anal. Calcd for $C_{42}H_{60}N_4O_2Cl_2\cdot 2.8H_2O$: C, 65.15; H, 8.54; N, 7.24. Found: C, 65.19; H, 8.26; N, 7.15.

(17) (a) Takahashi, K.; Hattori, K.; Toda, F. *Tetrahedron Lett.* **1984**, *25*, 3331–3334. (b) Ikeda, H.; Nagano, Y.; Du, Y.; Ikeda, T.; Toda, F. *Tetrahedron Lett.* **1990**, *31*, 5045–5048.

(18) Miyawaki, A.; Miyauchi, M.; Takashima, Y.; Yamaguchi, H.; Harada, A. *Chem. Commun* **2008**, *4*, 456–458.

4.3. Measurements. The NMR spectra were recorded on a JEOL JNM LA-500 and VARIAN UNITY600 NMR spectrometer. The preparative reversed phase chromatography was carried out with a Waters Delta 600 system (column: SunFireTM Prep C18 19 mm × 150 mm). Positive-ion matrix assisted laser desorption ionization time-of-flight (MALDI-TOF) mass spectrometry experiments were performed using a Shimadzu/KRATOS Axima CFR Ver.2.2.3 mass spectrometer calibrated by α-cyano-4-hydroxycinnamic acid and insulin. Photo irradiation was performed using a ASAHI SPECTRA xenon light source MAX-301 with a band-pass filter HQBP300-UV ϕ25.

4.3.1. PFGSE NMR Experiments. The PFGSE NMR diffusion measurements were carried out by using the bipolar pulse pair stimulated echo (BPPSTE).[19] The strength of the pulsed gradients was increased from 6.36×10^{-1} to 61.7 gauss/cm. The time separation of pulsed field gradients and their duration were 0.10 and 1.0×10^{-3} s. The sample was not spun, and the airflow was disconnected. The shape of the gradient pulse was rectangular, and its strength varied automatically during the course of the experiments. The D values which represent diffusion coefficient were determined from the slope of the regression line ln (I/I_o) versus G^2, according to following equation.

$$\ln(I/I_o) = -\gamma^2 G^2 \delta^2 (\Delta - \delta/3 - \tau/2) D$$

where (I/I_o) is (observed spin echo intensity/intensity without gradients), G is gradient strength, Δ is delay between the midpoints of the gradients, δ is gradient length, and τ is 90°−180° pulse distance. The calibration of the gradients was carried out by a diffusion measurement of H_2O ($D_{H2O} = 2.30 \times 10^{-9}$ m^2 s^{-1})[20] at 25 °C.

4.3.2. EXSY Experiments. The EXSY measurements[21] were carried out at 303 K with a phase-sensitive NOESY pulse sequence. The mixing time was increased from 100 to 900 ms. The k values, which represent rate constants, were determined by using the following equations.

$$A \underset{k_{off}}{\overset{k_{on}}{\rightleftarrows}} B$$

$$k = k_{on} + k_{off}$$

$$k = (1/\tau_m) \ln(r + 1/r - 1)$$

where τ_m is the mixing time and r is defined by the following equation

$$r = 4X_A X_B (I_{AA} + I_{BB})/(I_{AB} + I_{BA}) - (X_A - X_B)^2$$

where X_A and X_B are the mole fraction of A and B, respectively, I_{AB} and I_{BA} are the intensities of the cross peaks between the signals A and B, respectively, and I_{AA} and I_{BB} are the intensities of the diagonal signals. The free energy of activation of the interconversion was obtained from the Eyring equation

$$k = (k_B T/\hbar) \exp(-\Delta G^{\ddagger}/RT)$$

where k_B is the Boltzmann constant, T is the absolute temperature, $\hbar$ is Plank's constant, $\Delta G^{\ddagger}$ is the free energy of activation, and R is the gas constant.

4.3.3. UV−Vis Experiments. UV−vis measurements were carried out at room temperature. The absorbance at 280 nm was measured for 10 min after dissolving the sample in water at 0.1 mM. The noninclusion (α state) sample for these experiments was prepared by precipitation from methanol to acetone. The k values, which represent rate constant, were determined by fitting the absorbance decay in following equations.

$$A \underset{k_{off}}{\overset{k_{on}}{\rightleftarrows}} B$$

$$k = k_{on} + k_{off}$$

$$\tau = 1/(k_{on} + k_{off})$$

$$\mathrm{Abs} = r(1 - \exp(-t/\tau))$$

where K is self-assembly constant, Abs is the absorbance at 280 nm, t is time, τ is relaxation time, and r is defined by the following equation

$$r = (k_{on}a - k_{off}b)/(k_{on} + k_{off})$$

where a is initial concentration of A and b is initial concentration of B. In the case of self-complexation for **1-Ad**, the K value was determined to be $K = 1$ from the ^{1}H NMR spectrometry measurement; hence

$$\tau = 1/(2k_{on})$$

4.4. Calculated Structures. Quantum-chemical calculations were performed by employing the Spartan '06 package on a 32-bit multiprocessor computer. Semiempirical (AM1) method geometrical optimization was carried out for calculating molecular volume of substituents. The Hartree−Fock (HF) geometrical optimization was carried out with the 3-21G basis set for determination of 3-NH_2-*altro*-α-CD ($^1C_4$ and $^4C_1$), and α-CD structures. To account for solvent effects, calculations were performed in the presence of water molecules.

Acknowledgment. We thank Dr. A. Hashidzume and Mr. Seiji Adachi, Osaka University for his helpful comments and NMR experiments. This work has been partially supported by global COE program and Grant in-Aid No. A19205014 for Scientific Research. A.M. and P.K. acknowledge JSPS for financial support (20 • 637 and 19 • P07064).

Supporting Information Available: UV−vis, PFGSTE NMR, ^{1}H NMR, ROESY, EXSY, van't Hoff plot, and calculated structures.This material is available free of charge via the Internet at http://pubs.acs.org.

JA806620Z

(19) (a) Stejskal, O. E; Tanner, J. E. *J. Chem. Phys.* **1965**, *42*, 288–292. (b) Stilbs, P. *Prog. in NMR Spectrosc.* **1987**, *19*, 1–45.
(20) Weingartner, H. *Z. Phys. Chem. (Leipzig)* **1982**, *132*, 129–149.
(21) Perrin, C. L.; Dwyer, T. J. *Chem. Rev.* **1990**, *90*, 935–967.